

Energy Efficient Multimedia Delivery Services over LTE/LTE-A

Chadi KHIRALLAH[†], Dragan RASTOVAC^{††}, Nonmembers, Dejan VUKOBRATOVIĆ^{††a}, Member,
and John THOMPSON[†], Nonmember

SUMMARY Mobile video services are becoming a dominant traffic category in emerging fourth generation (4G) cellular networks such as the 3GPP Long-Term Evolution (LTE) and LTE-Advanced (LTE-A). In particular, mobile video unicasting services based on 3GPP Dynamic Adaptive Streaming over HTTP (DASH) and multicasting/broadcasting services based on 3GPP evolved Multimedia Multicast/Broadcast Service (eMBMS) will require considerable resources for high-quality service delivery with high coverage probability. Faced with the challenge of energy efficient multimedia service provisioning over LTE/LTE-A, in this paper, we present simple analytical tools for evaluation of average service data rates, bandwidth and energy-consumption requirements applicable for different multimedia delivery services and LTE/LTE-A radio access network (RAN) configurations. Moreover, we introduce and evaluate novel energy and bandwidth performance measures defined *per unit of service*. As a result, we are able to compare the efficiency of different multimedia service delivery configurations over LTE/LTE-A. In particular, in this paper, as a running example we focus on eMBMS and compare the *Energy of Service (EoS)* of the two macro-cellular LTE/LTE-A configurations recently proposed in 3GPP: i) a single frequency network eMBMS (SFN-eMBMS), and ii) a single-cell eMBMS (SC-eMBMS). Furthermore, we extend this analysis to eMBMS provisioning over Heterogeneous Networks (HetNets) environment. However, the methodology presented is general and targets light-weight system design and comparison of bandwidth/energy costs of different LTE/LTE-A multimedia service delivery configurations.

key words: eMBMS, energy efficiency, video multicast, LTE/LTE-A

1. Introduction

The dramatic increase in the predicted volume of wireless Internet traffic can be attributed to mobile multimedia applications. This is recently confirmed by the Cisco Visual Networking Index estimate that mobile data traffic will increase 13-fold in the period 2012–2017 [1]. Provisioning of high-quality multimedia services over cellular networks has become a reality as a result of technological maturity reached at both the cellular network and the user equipment (UE) side. Indeed, the requirements for high quality multimedia over cellular are met with the introduction of 3GPP Long Term Evolution (LTE) and LTE-Advanced (LTE-A) [2], [3]. In addition, typical smartphones/tablets available on the market represent powerful handheld computers able to process high-quality compressed multimedia and present

it on a large size/resolution screen. This trend of video traffic domination in the mobile cellular Internet opens a great challenge for mobile network operators. Providing sufficient network capacity that meets growing traffic demands while preventing the operational expenditure and energy requirements of the network from scaling directly with traffic volumes present conflicting demands.

In this paper, we address the energy and spectrum efficient design and analysis of multimedia service delivery over LTE/LTE-A. We introduce a simple framework for evaluation of average service data rates, bandwidth and energy-consumption requirements for multimedia service provisioning in LTE/LTE-A. In the proposed framework, average service data rates are evaluated based on Finite-State Markov Chain (FSMC) modeling of user channels [4] customized to the LTE/LTE-A physical-layer, in combination with the fixed coverage probability service requirements. Moreover, we introduce novel bandwidth and energy performance measures defined *per unit of service* suitable for system design and comparison of service delivery efficiency of different LTE/LTE-A configurations. In particular, we focus on the mobile video broadcasting service, 3GPP evolved Multimedia Multicast/Broadcast Service (eMBMS) [5], [6], as a running example. For example, in the specific eMBMS LTE/LTE-A scenario, introducing energy costs per eMBMS service channel sets the ground for *Energy of Service (EoS)* definition, investigation and comparison of different eMBMS over LTE/LTE-A configurations. To provide the proof-of-concept for our approach, we evaluate the bandwidth and energy efficiency of eMBMS provisioning under varying Quality of Experience (QoE) requirements over two LTE/LTE-A macro-cellular configurations recently proposed in 3GPP. These are a single frequency network eMBMS (SFN-eMBMS) and a single-cell eMBMS (SC-eMBMS) configuration [6]. Furthermore, we extend this analysis to eMBMS provisioning over more interesting and dynamic Heterogeneous Network (HetNets) environment [7]. However, we note that the results and methodology introduced in this paper are general and could be extended for comparison of different LTE/LTE-A multimedia delivery services over various upcoming heterogeneous LTE (HetNets) network configurations.

The rest of the paper is organized as follows. Section 2 provides background on 3GPP defined multimedia delivery services in LTE/LTE-A. In Sect. 3, we provide a system model for video delivery services based on FSMC

Manuscript received January 11, 2014.

[†]The authors are with the School of Engineering and Electronics, The University of Edinburgh, Edinburgh, UK.

^{††}The authors are with the Department of Power, Electronics and Communication Engineering, University of Novi Sad, Novi Sad, Serbia.

a) E-mail: dejany@uns.ac.rs

DOI: 10.1587/transcom.E97.B.1504

modeling of the LTE downlink transmission process. Focusing on eMBMS service, in Sect. 4 we derive average rate vs. coverage probability analysis for the SFN and SC-eMBMS configurations. Section 5 presents bandwidth and energy efficiency analysis per video service unit. These are applied in Sect. 6 to SFN and SC-eMBMS providing their bandwidth/energy service cost evaluation and comparison while taking the QoE into account. The paper is concluded in Sect. 7.

2. Background

In this section, we provide brief overview on: i) the IP content delivery to mobile users via LTE/LTE-A interface, and ii) the most popular 3GPP-standardized multimedia delivery services over LTE/LTE-A.

2.1 3GPP LTE/LTE-A RAN Protocols

The LTE standard provides efficient broadband wireless IP connectivity between the base station (eNB - eNodeB) and the mobile UE through the new evolved UMTS terrestrial Radio Access Network (E-UTRAN) architecture introduced in 3GPP LTE Release 8 [8]. Figure 1 illustrates the protocol stack responsible for the downlink (DL) IP packet flow at the eNB/UE interface.

IP packets enter the eNB through the Packet Data Conversion Protocol (PDCP). After header compression and ciphering, PDCP encapsulated IP packets (IP/PDCP) are delivered to the Radio Link Control (RLC) layer. The RLC layer performs segmentation/concatenation of IP/PDCP packets into RLC packets to fit the MAC frame size requirements, which are in turn selected to fit the physical layer (PHY) transport block (TB) sizes. Thus each MAC frame is allocated a single PHY TB for transmission over the eNB/UE interface. For unicast transmission, reliable MAC frame delivery over the eNB/UE link is supported by the MAC/PHY layer HARQ mechanism. If HARQ fails, the RLC-layer ARQ mechanism may be (optionally) used to guarantee reliable RLC packet delivery [9], [10].

The PHY TB represents a PHY packet whose size (TBS) within a single transmission time interval (TTI) depends on: i) the modulation/coding (MC) scheme selected by the MAC-layer scheduler based on the Channel Quality Indicator (CQI) reported by the UE, and ii) the amount of PHY resource blocks (RBs) allocated to the UE. The PHY RB represents a unit of time-frequency resources: 0.5 ms time duration ($\frac{1}{2}$ TTI) and 12 OFDM carriers (180 kHz) of bandwidth. PHY RBs are always allocated in pairs, thus the PHY TBS depends on the number N_{RBP} of RB pairs (RBPs), $1 \text{ RBP} = 180 \text{ kHz} \times 1 \text{ TTI}$, allocated to the UE and the CQI value fed back by the UE (see Table 1, TBS column for the case $N_{RBP} = 6$, i.e., a Category 1 LTE user). For more details on the LTE RAN protocols, we refer the reader to [8]–[10].

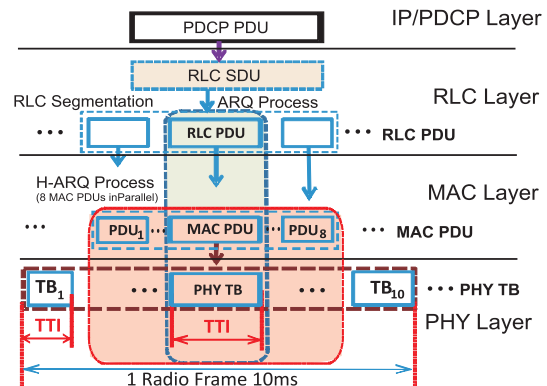


Fig. 1 eNB DL packet flow from IP to PHY layer.

Table 1 CQI values and the corresponding TB sizes.

CQI index	modulation	code rate	bits per symbol	SINR (dB)	TBS (bits)
0 – 3	No Tx	-	-	< -1.25	0
4	QPSK	0.3	0.6016	-0.94	384
5	QPSK	0.44	0.8770	1.09	576
6	QPSK	0.59	1.1758	2.97	768
7	16QAM	0.37	1.4766	5.31	960
8	16QAM	0.48	1.9141	6.72	1152
9	16QAM	0.6	2.4063	8.75	1536
10	64QAM	0.45	2.7305	10.47	1920
11	64QAM	0.55	3.3223	12.34	2304
12	64QAM	0.65	3.9023	14.37	2688
13	64QAM	0.75	4.5234	15.94	3072
14	64QAM	0.85	5.1152	17.81	3456
15	64QAM	0.93	5.5547	20.31	3840

2.2 Multimedia Delivery Services over LTE/LTE-A

3GPP standards for multimedia delivery over LTE/LTE-A define two categories for video delivery services: the adaptive HTTP streaming service (DASH) that targets unicast media streaming to small group of users [11], and the eMBMS suitable for broadcasting the same video content to a large number of users over a common radio channel [5].

Dynamic adaptive streaming over HTTP (DASH) for the progressive download of video content has gained popularity due to low operational costs and bandwidth requirements, dynamic bit rate adaptation and improved scalability [11]–[13]. DASH is a segment-based streaming solution in which segments of the media content are provided by server in multiple representations that differ in video bit rates, frame rates, resolution, and quality. All the decisions are moved from servers to clients thus liberating servers from large dependencies on different devices, while enabling each client to adjust streaming session to its own abilities. This is done by allowing users to dynamically choose the segment of highest quality according to its currently experienced network conditions and handset capabilities [12].

3GPP standard allowing for point-to-multipoint multimedia transmission (MBMS) has been defined starting from Release 6 [6]. In Release 8 [8], the enhanced MBMS (eM-

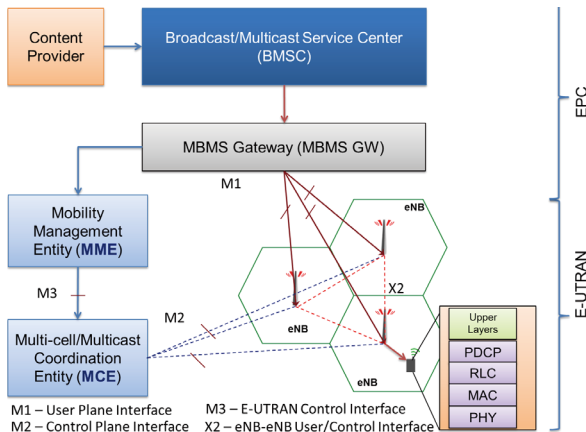


Fig. 2 3GPP eMBMS System Architecture.

BMS) design is introduced with two proposed transmission schemes. The first one, single-cell (SC-eMBMS) transmission, overcomes pre-LTE MBMS shortcomings by allowing user feedback on channel conditions and dynamic selection of the suitable MC scheme. The advantage of this scheme is dynamic adaptation to current distribution of users in the cell. Furthermore, in terms of energy efficiency, the SC-eMBMS service can be turned-off in the cells with no active service. The second one, multicell or so called single frequency network (SFN-eMBMS) transmission, represents a coordinated effort of macro eNBs to cover the network with the same physical signal, where a fixed MC scheme adapted to match the worst-case edge-user requirements is applied. SFN-eMBMS results in increased achievable rates at the cell edge [14]. In contrast to SC-eMBMS, SFN-eMBMS is fixed and designed in advance and does not depend on the user distribution over the cells [6].

The eMBMS system architecture is presented in Fig. 2. For SC-eMBMS, it reuses similar architecture as for the standard LTE unicast service with the eMBMS service gateway (MBMS GW) and the Mobility Management Entity (MME). SFN-eMBMS requires additional coordination within single frequency network of eNBs, which is maintained by Multi-cell multicast Coordination Entity (MCE). Service-level entity called Broadcast/Multicast Service Center (BMSC) maintains service activation and session management between service users and the content provider. Detailed description of the eMBMS architecture and system interfaces is available in [15].

3. System Model for Multimedia Delivery Services over LTE/LTE-A

Mobile multimedia services are delivered to cellular users encapsulated into IP data streams. IP packets are transmitted via the eNB/UE radio-interface over frequency/time resources consisting of a set of PHY RBs allocated over a time-sequence of TTI slots. Accurate modeling of instantaneous channel conditions and achievable data rates as seen by UEs at various cell locations is fundamental for efficient

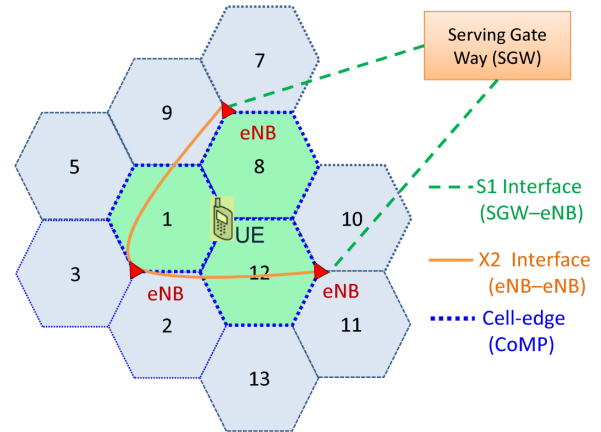


Fig. 3 LTE/LTE-A system model for SFN and SC-eMBMS.

design of multimedia delivery services over LTE/LTE-A.

3.1 LTE/LTE-A System Model

We consider a LTE/LTE-A system model consisting of a macro-cellular site that combines 19 macro-cell eNBs arranged in two tiers around a central eNB (Fig. 3 illustrates part of the layout).

For a UE placed at a distance d from the eNB, the average Signal-to-Interference-and-Noise Ratio (SINR) at the UE is [8]:

$$SINR(d) = P_{TX} + G_{TX} + G_{RX} - N - I - S(d) - PL(d) - PNL, \quad (1)$$

where P_{TX} is the eNB transmission power (per cell sector); G_{TX} and G_{RX} are the eNB and the UE antenna gains (including 3GPP defined horizontal and vertical antenna patterns); N and I are the noise and the ICI power from all the interfering eNBs at the UE location; PNL is the wall penetration loss for signals received at indoor UEs; and finally, S and PL are the shadowing loss and the pathloss in dB measured at different UE positions using shadowing variances and pathloss models defined in Table 2 following [8].

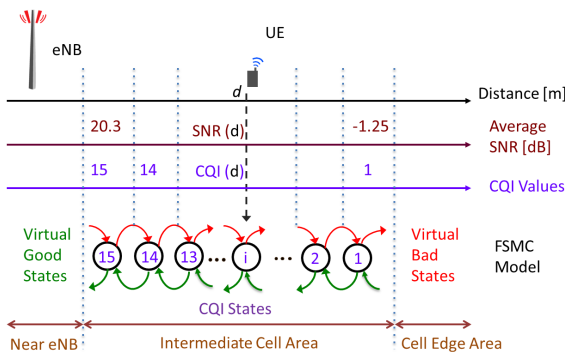
3.2 LTE/LTE-A Downlink Packet-Level Channel Model

The PHY TB transmission process underlies the multimedia IP services over LTE E-UTRAN. Thus in this section, we derive a simple model of the PHY TB transmission in order to provide reasonable estimates of achievable data rates for UEs located within the cell domain.

The PHY TB transmission process model requires: i) the description of the process of CQI values reporting as seen by the eNB, and ii) PHY TB error rate estimates for different CQI values as seen from the MAC layer. It seems natural to model the reported CQI values and their dynamics using Finite-State Markov Chain (FSMC) channel models [4]. For simplicity, assuming Rayleigh fading statistics and a fixed PHY RB frequency allocation over time (TTIs)

Table 2 LTE/LTE-A parameters and system assumptions.

Parameter	Value
Inter site distance (ISD)	500 m (3GPP Case 1)
Traffic model	Downlink full buffer
Duplexing mode	FDD
System bandwidth	2×40 MHz (LTE-A)
eMBMS service allocation	25%
Subcarrier spacing	7.5 kHz
Number of usable data RBs/TTI	100 RBPs per 10 MHz
OFDMA useful symb duration	0.133 ms
Number of OFDMA symb/frame	6 per subframe
Number of RBPs per TTI	100 RBPs
MBMS control overhead	10%
Transmission scheme	SISO
Frame duration	10 ms
Carrier frequency	2.0 GHz
System layout	multi-cell (19 macro-cells) - Het-Nets (micro+pico cells)
Pathloss	eNB-UE 3GPP model
Penetration loss (PNL)	20 dB
Shadowing (macro,micro,pico)	Shadow fading: Log normal - stdev eNB-UE:(10, 10, 6) dB
Terminal speed	3 km/h
Max Tx power: macro,micro,pico	eNB:(46, 22, 16) dBm/sector
Max Antenna gain: macro,micro,pico	eNB:(14, 9, 5) dBi, UE:0 dBi
Antenna height: macro,micro,pico	eNB:(25, 5, 1.5) m, UE:1.5 m
Noise figure	UE:7 dB
Max. HARQ retransmissions	3

**Fig. 4** FSMC model of PHY TB transmission process.

with sufficiently low user mobility and multipath signal dispersion, the packet-level PHY TB channel can be modeled using slowly-varying frequency-flat Rayleigh fading FSMC models [16], [17]. We customize these models for our purpose: for LTE/LTE-A, the SINR division into FSMC states is naturally provided by the SINR intervals defining different CQI values (Table 1, SINR column). Thus we “embed” the LTE division of SINR axis into the FSMC model in [17]. To embed the CQI states into the FSMC model, for UEs close to the eNB or the cell-edge, we dynamically introduce an additional set of “virtual” states. *Virtual good states* are introduced for SINRs larger than the CQI 15 (SINR > 20.31 dB) state and are assumed to deliver maximum size PHY TBs without errors (BLER=0); *Virtual bad states* are introduced for SINRs lower than the CQI 0 state (SINR < -1.25 dB), and are assumed to result in PHY TB transmission failure (BLER=1), as illustrated in Fig. 4.

Based on the average $SINR(d)$ at the UE calculated using (1) and the SINR intervals of CQI states, we establish an FSMC model representing the CQI state reporting process for any given UE location. Using the FSMC model, one can easily derive the set $\pi = \{\pi_1, \pi_2, \dots, \pi_{N_{CQI}}\}$ of steady state probabilities of N_{CQI} CQI states using the expressions in [17]. While in the i -th CQI state, the average data rate achievable at the UE equals:

$$R_i = \frac{TBS(i) \cdot N_{RBP}}{TTI} (1 - BLER(i)), \quad (2)$$

where $TBS(i)$ is the PHY TB information capacity (in bits, Table 1, TBS column) and $BLER(i)$ is the average BLER for the CQI state i . We calculate the $BLER(i)$ by weighted averaging of simulated PHY TB BLERs over N_S substates (equidistant SINR points) within the SINR interval of the i -th CQI state:

$$BLER(i) = \sum_{j=1}^{N_S} P(j) \cdot BLER^{(sim)}(j). \quad (3)$$

$P(j)$, $1 \leq j \leq N_S$, is the substate probability distribution, obtained from the instantaneous SINR probability distribution law normalized to the SINR interval of the i -th CQI state [17]. $BLER^{(sim)}(j)$ is the j -th substate BLER obtained by LTE PHY simulations [18]. Finally, the average rate $R_{avg}(d)$ of PHY TB data delivery to the UE placed at the distance d from the eNB:

$$R_{avg}(d) = \pi \cdot \mathbf{R}^T, \quad (4)$$

where $\mathbf{R} = \{R_1, R_2, \dots, R_{N_{CQI}}\}$. Note that these rates correspond to unicast transmission, where the eNB continuously adapts the MC scheme to the UE reported CQI values, and are thus applicable for DASH service analysis. However, the same approach is reusable for broadcast transmission, where the eNB applies fixed MC scheme. In that case, assuming the eNB applies the MC scheme corresponding to the CQI value s , the values in \mathbf{R} are: $R_i = R_s$, for all $i \geq s$, and $R_i = 0$ otherwise. In other words, the UEs that report CQI values greater than or equal to s will receive the fixed service rate R_s , while those below this CQI value will fail to receive data.

4. eMBMS: Average Rates vs. Coverage Probability

As a running example, in this paper we focus on the energy-efficiency analysis of eMBMS services. We assume eMBMS services are provided over a fraction of system frequency resources (e.g., fixed set of allocated PHY RBs), using either SC-eMBMS or SFN-eMBMS.

For SFN-eMBMS, we assume that perfectly coordinated and synchronized set of eNBs jointly transmit the same physical signal to the UEs in the cell domain.

The ICI factor I in SINR-equation (1) depends on which of the two eMBMS strategies are in use. For SC-eMBMS, the received signal power from all the eNBs except

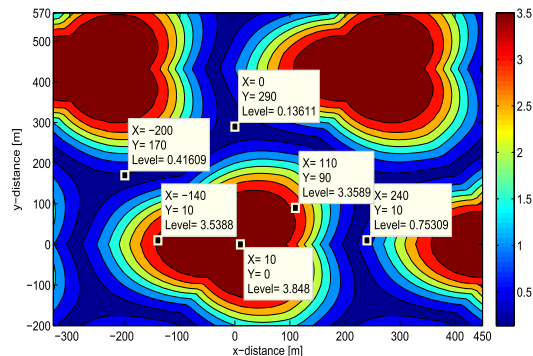


Fig. 5 Average rate (Mbits/s) per user located in the central eNB cell domain when eNBs transmit different PHY signals (SC-eMBMS).

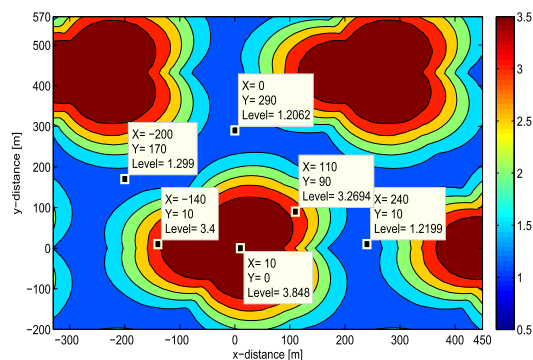


Fig. 6 Average rate (Mbits/s) per user located in the central eNB cell domain when eNBs transmit the same PHY signals (SFN-eMBMS).

the strongest one contributes to the ICI factor. For SFN-eMBMS, neighboring eNBs support each other by coherently transmitting the same signal over the same frequency resource. Due to synchronization complexity, we assume the cluster of 3 strongest eNBs provide useful signal matching while other eNBs contribute to the ICI factor.

Before proceeding, it is useful to observe Figs. 5 and 6. These figures present average data rates (in Mbits/s) calculated using Eq. (4) across the area of the central eNB under assumptions that neighboring eNBs transmit different PHY signals (Fig. 5), which is the case for SC-eMBMS, or that neighboring eNBs transmit the same signal (Fig. 6), which is the case in SFN-eMBMS. Clearly, by inspecting the numbers provided for example positions at the cell-edge area, we can observe that SFN-eMBMS benefits from signal superposition which affects the reception quality in the cell edge domain. On the other hand, the strict constraint that the PHY signals delivered from eNBs should be the same significantly restricts the flexibility as compared to the SC-eMBMS service.

4.1 SFN-eMBMS: Average Rate vs. Coverage Probability

The SFN-MBMS is delivered from all eNBs using the same set of PHY parameters selected to meet the desired cell coverage probability threshold $P_{th}^{(cov)}$ (the service coverage probability is defined as the probability that a uniformly and ran-

domly placed UE achieves the SINR threshold required by the service). In general, exact coverage probability calculations are hard [19], thus we use approximations following from the FSMC modeling to obtain reasonable estimates.

Let us reformulate the coverage probability problem for the scenario and model we observe. We assume the eNB broadcasts the service using a fixed MC scheme corresponding to CQI value s selected in advance. For any UE in the cell, the average received SINR is known (see Sect. 3). Feeding the FSMC model with the average SINR, we obtain the set π of steady CQI state probabilities at the UE. The coverage probability $P_{UE,s}^{(cov)}$ is:

$$P_{UE,s}^{(cov)} = \sum_{i \geq s} \pi_i. \quad (5)$$

Averaging the $P_{UE,s}^{(cov)}$ over the cell area, we obtain the (cell) coverage probability. For simplicity, we introduce two assumptions: i) the average SINR is circularly symmetric with respect to the eNB, and ii) the cell area represents a circle of radius r_c . The first assumption restricts attention to any radial line emanating from the eNB; we select the worst-case radial line in terms of SINR values thus lower-bounding the coverage probability. For the second assumption, we use the circle of minimum radius that covers all UEs connecting to the eNB. Finally, the coverage probability is approximated by a ‘‘Riemann-like’’ weighted sum of coverage probabilities at points located at a sequence of N_r concentric rings defined by the set of equidistant radii $\mathbf{d} = \{d_1 = 0, d_2, \dots, d_{N_r+1} = r_c\}$, where $d_{i+1} - d_i = r_c/N_r$. The cell coverage probability is:

$$P_{cell,s}^{(cov)} = \sum_{i=1}^{N_r} P_h(d_i : d_{i+1}) \cdot P_{UE}^{(cov)}(d_{i+1}), \quad (6)$$

where $P_h(d_i : d_{i+1}) = (d_{i+1}^2 - d_i^2)/r_c^2$ is the probability that a UE, placed uniformly and randomly within the circular cell area of radius r_c , hits the ring defined by $[d_i, d_{i+1}]$. For the desired coverage probability threshold $P_{cell,th}^{(cov)}$, the SFN-MBMS should broadcast using the highest CQI value s^* for which the coverage probability $P_{c,s^*}^{(cov)}$ exceeds $P_{cell,th}^{(cov)}$:

$$s^* = \max\{s \in CQI : P_{cell,s}^{(cov)} \geq P_{cell,th}^{(cov)}\}, \quad (7)$$

where CQI represents the set of indices of CQI states. Thus, the SFN-MBMS is able to achieve the average rate:

$$R_{s^*}^{SFN} = \frac{TBS(s^*) \cdot N_{RBP}}{TTI} (1 - BLER(s^*)), \quad (8)$$

while satisfying the $P_{cell,th}^{(cov)}$ requirement.

4.2 SC-eMBMS: Average Rate vs. Coverage Probability

The rationale of the SC-eMBMS is that a small number of users in the cell is likely to be able to receive better service than the one used by the SFN-MBMS service [6]. In the following, assuming a Poisson distribution of UEs with intensity λ , we derive the average rate of the SC-MBMS for a

given coverage probability $P_{cell,th}^{(cov)}$.

We start with the inverse problem from the one discussed for SFN-MBMS: given $P_{cell,th}^{(cov)}$ and fixed CQI state s , we search for the radius r_s such that if the eNB transmits using the MC scheme for the CQI state s , the UEs within the circle of radius r_s will receive the service with $P_{cell,s}^{(cov)} \geq P_{cell,th}^{(cov)}$. By increasing the CQI state values s between $s^* < s < N_{CQI}$, where s^* is the CQI state that covers the whole cell, we obtain the set of radii $\mathbf{r} = \{r_{N_{CQI}}, r_{N_{CQI}-1}, \dots, r_{s^*+1}\}$, each of which defines the $P_{cell,th}^{(cov)}$ coverage probability region for the corresponding CQI state. For example, for CQI state s , we obtain r_s using slightly altered version of equation (6):

$$P_{cell,s}^{(cov)} = \sum_{i=0}^n P_h(d_i : d_{i+1}) \cdot P_{UE}^{(cov)}(d_{i+1}), \quad (9)$$

where in the above equation, what we aim to evaluate is n . More precisely, we increase n thus increasing the set of equidistant rings defined by their radii $\mathbf{d} = \{d_1 = 0, d_2 = \delta, d_3 = 2\delta, \dots, d_n = (n-1)\delta\}$ in a ring-by-ring fashion until the coverage probability $P_{cell,s}^{(cov)}$ exceeds $P_{cell,th}^{(cov)}$:

$$n(r_s) = \min\{n \in \mathbb{N} : P_{cell,s}^{(cov)} \geq P_{cell,th}^{(cov)}\}. \quad (10)$$

Depending on the selected radius increment δ , we get arbitrary good estimate of $r_s = n(r_s) \cdot \delta$.

Using \mathbf{r} and the user density λ , we calculate the probability that there are exactly i users in the cell, and all of them reside within the radius r_j . In SC-MBMS setup, this is the probability that, given there are i users in the cell, the eNB broadcasting at rate R_j defined by the MC scheme of the CQI state j , will cover all the UEs with probability $P_{cell,th}^{(cov)}$. Averaging the achievable eNB rates across the possible number of users in the cell and the possible CQI state coverage radii, we obtain the average SC-MBMS rate:

$$R^{SC}(\lambda) = \sum_{i=1}^{N_u} \sum_{j=s^*}^{N_{CQI}} P_\lambda(i) \cdot P_h(i, r_j) \cdot (1 - P_h(i, r_{j+1})) \cdot R_j. \quad (11)$$

In the expression above, $P_\lambda(i)$ describes the Poisson distribution:

$$P_\lambda(i) = \frac{(\lambda A)^i}{i!} \exp(-\lambda A), \quad (12)$$

describing the number i of cell users as a function of the average user density λA , where A is the cell area, and i is limited to some sufficiently large value N_u . $P_h(i, r_j)$ is the probability that i UEs, placed uniformly and randomly within the circular cell area, simultaneously hit the circle defined by the radius r_j :

$$P_h(i, r_j) = \left(\frac{r_j}{r_c}\right)^{2i}. \quad (13)$$

Finally, R_j is the average rate achievable by the covered UE

obtained from Eq. (2). For the expression (11), it is important to note that the eNB will transmit using the rate R_j if all the users are confined within the ring r_j , but not all of them are confined to a smaller ring r_{j+1} (otherwise, the eNB would increase the transmission rate to R_{j+1}). Note also that, unlike R_s^{SFN} , the average rate for the SC-MBMS service $R^{SC}(\lambda)$ depends on the user distribution through the average number of users per unit area λ .

5. Bandwidth and Energy Efficiency Evaluation of eMBMS in LTE/LTE-A

Given the average data rates available for video broadcast service delivery for different modes of system operation, we derive system utilization parameters in terms of bandwidth usage and energy consumption. These parameters are calculated *per unit of service*, which in our scenario represents a constant bitrate eMBMS video channel. The energy efficiency evaluation of eMBMS service units relies on energy consumption models of eNBs. The resulting energy per channel metric could be understood as a novel *Energy of Service (EoS)* parameter. The EoS could be fundamental for evaluation and comparison of different service architectures and selection of optimal ones with respect to the total energy costs service unit that satisfies specific QoE-based user requirements, as detailed below.

5.1 Capacity and Bandwidth Costs of eMBMS

Given the average service rate, the average number of eMBMS video channels for a given system configuration is obtained similarly as in [3]:

$$N_{eMBMS}^{cfg} = \frac{N_{RBP}^{(DL)} \cdot F_{eMBMS}^{(DL)} \cdot (1 - \alpha_{eMBMS}) \cdot R_{th\%}^{cfg}}{R_{eMBMS}}. \quad (14)$$

In the above equation, $N_{RBP}^{(DL)}$ represents the number of PHY RBPs allocated for MBMS video delivery service, $F_{eMBMS}^{(DL)}$ is the fraction of frame symbols allocated for eMBMS, α_{eMBMS} is a fraction of control data required by eMBMS ($\alpha_{eMBMS} = 10\%$ [3]), $R_{th\%}^{cfg}$ is the average data rate of the *cfg* system configuration (*cfg* could be SFN-eMBMS or SC-eMBMS service configuration) required to achieve *th%* user coverage, and finally, R_{eMBMS} is the service unit data rate: a single eMBMS channel (e.g., 384, 768 or 1536 kbps) [3]. From the number of eMBMS channels the system configuration is able to provide over a given frequency allocation $N_{RBP}^{(DL)}$, the bandwidth allocation (in kHz) per eMBMS channel is:

$$B_{MBMS}^{cfg} = \frac{N_{RBP}^{(DL)} \cdot 180}{N_{MBMS}}. \quad (15)$$

5.2 Energy Efficiency of eMBMS

To investigate the energy efficiency of SFN and SC-eMBMS in a LTE/LTE-A, we first define a suitable macro eNB power

consumption model, from which we directly obtain the energy costs per eMBMS channel. In general, macro eNB power models consist of dynamic and static components. While the dynamic part varies with the eNB average transmission power and the instantaneous traffic load, the static part (or zero-load) is independent of these parameters and represents the power consumption in equipment such as the transceiver (base-band and radio), climate control (cooling sections) and interfaces [20]–[23].

In [22], the macro eNB power model describes the relation between the eNB operational power P_{Op}^{eNB} and its maximum transmission power $P_{Tx,max}^{eNB}$ as given by:

$$P_{Op}^{eNB} = \alpha P_{Tx,max}^{eNB} \cdot l + \beta, \quad (16)$$

where P_{Op}^{eNB} and $P_{Tx,max}^{eNB}$ are given in Watts (W), l is the value of the traffic load that varies between 0 (no load) and 1 (full-load), α is a constant that accounts for the power efficiency of the eNB power amplifier (PA), power supply unit, etc, while β is the zero-load macro eNB power consumption. In this paper, we choose $\alpha = 2.85$ and $\beta = 602$ W, based on available energy-efficiency figures for state-of-the-art macro eNB components [24].

From the number of eMBMS channels that the system provides over a given frequency allocation $N_{RBP}^{(DL)}$, it is easy to obtain the energy (or power) cost per eMBMS channel:

$$P_{MBMS}^{cfg} = \frac{P_{Op}^{eNB} \cdot N_{RBP}^{(DL)}}{N_{MBMS}^{(tot)}}. \quad (17)$$

where $N_{MBMS}^{(tot)}$ is the total number of resource blocks.

5.3 Extension to eMBMS over LTE/LTE-A HetNets

With the ongoing evolution from macro-cellular to Heterogeneous Networks (HetNets), the potential for offering higher-quality video services increases. Thus HetNets based evolved E-UTRAN offers novel opportunities for enhancements in mobile video delivery services including eMBMS through, e.g., service “offloading” from macro cells to small cells or dynamic power control (“cell-zooming”) of small cells. On the other hand, E-UTRAN energy efficiency becomes major concern as introduction of small cells places additional burden on E-UTRAN power consumption.

We further extend our SC-eMBMS service analysis assuming service traffic is offloaded to small cells whenever a mobile user equipment (UE) that consumes the service experiences better connection via a neighbouring small cell eNBs compared to the connection towards macro eNB. We assume a given number of micro and pico eNBs is randomly placed according to Poisson point process. Each class of eNBs (macro, micro and pico) is allocated a separate and disjoint set of PHY RBs. We apply micro eNB power consumption model from [25] and pico eNB power consumption model from [26] (Sect. 3, Eq. (6), Table III).

6. Simulation Results

In this section, we provide the SFN and SC-eMBMS bandwidth and energy service costs evaluation and comparison in macro-cellular scenario. We also include simulation results of energy efficiency of SC-eMBMS delivery across LTE/LTE-A HetNets. Finally, we include QoE-based user requirements following from the suitable QoE models for H.264/Scalable Video Coding (SVC) [31] compressed video traffic into the proposed framework for system design and evaluation.

6.1 SC-eMBMS vs. SFN-eMBMS: Energy of Service

Using the FSMC-based system modeling methodology presented in Sect. 3.2, and applying the average service rate evaluation derived in Sect. 4.1, we are able to calculate the bandwidth and energy costs per service unit, as detailed in Sect. 5. More precisely, for the system layout and parameters introduced in Sect. 3.1 and Table 2, we used Eqs. (8) and (11) to calculate the average data rate R_s^{SFN} and $R_s^{SC}(\lambda)$ of both SFN and SC-MBMS configurations. The results obtained for SC-eMBMS are a function of the user density λ . Then, using expressions (15) and (17), we obtain the bandwidth and energy costs per fixed-rate MBMS channel for both configurations.

Figures 7 and 8 show the bandwidth and energy costs per downlink video broadcast channel of service rates equal

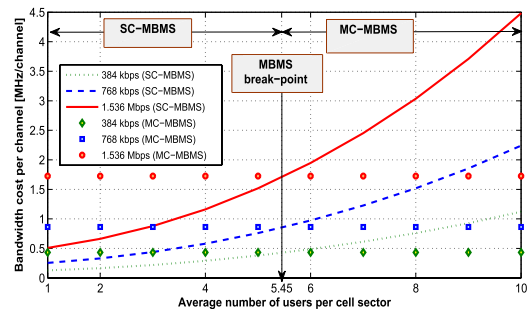


Fig. 7 SFN-eMBMS vs. SC-eMBMS: bandwidth cost per channel (MHz/channel).

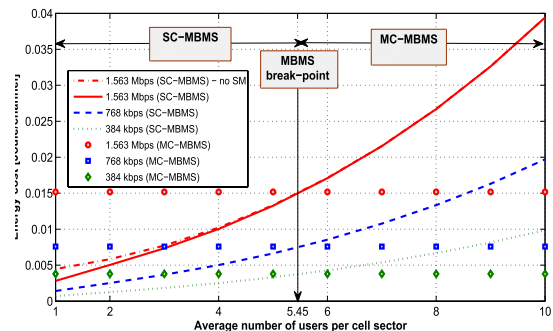


Fig. 8 SFN-eMBMS vs. SC-eMBMS: energy cost per channel (Joule/channel).

384, 768 and 1536 kbps for both the SFN-eMBMS and the SC-eMBMS transmission schemes. The results are parameterized by the average user density per cell λA and provide bandwidth costs in [MHz/channel] and energy costs in [J/channel] per channel (service unit) of the eMBMS service. The results provide for direct comparison of the two different LTE-A eMBMS configurations with respect to the bandwidth and energy of service costs. As can be seen from the results, the SC-eMBMS transmission scheme is more suitable at low user densities, in particular, for user density values less than 5.45 users/cell. In addition, the SC-eMBMS service allows for switching-off cells without eMBMS users to save energy, which is additionally emphasized in Fig. 8 for eMBMS channel rate of 1.536 Mbps (by factoring the energy costs with $P_{\lambda}(0)$). The SFN-eMBMS scheme is more efficient in providing improved cell-edge rates, which is reflected in its better performance at higher user densities. Finally, we note that the simple analytical tools proposed in this paper provide results that correspond very well to similar efforts reported within 3GPP [27]–[29], where the results are obtained through simulations.

6.2 SC-eMBMS Delivery over LTE/LTE-A HetNets

We extend the SC-eMBMS scenario by randomly placing N_{μ} , N_p and N_{UE} micro and pico cells and mobile users in the circular area of radius r_c within the coverage area of the central macro eNB cell. We assume that every UE selects the point of connection to be the eNB (either macro or small) that provides the highest average SINR. In each simulation run, we calculate the frequency resources that every eNB has to allocate in order to be able to offer an average eMBMS service rate of R [kbps]. In other words, we assume that each eNB (macro or small) is notified on all the UEs it serves and their respective SINR values. From this information the eNB extracts the worst-case user and, using Eqs. (2) and (4) as a function of N_{RBP} , calculates the minimum amount of frequency resources $N_{RBP}^{(eNB)}$ it has to allocate so that the worst-case user average rate R_{min}^{eNB} exceeds the service rate R . Finally, the total power eNB invested in the eMBMS is obtained by pondering the dynamic component of the total power expressions with the amount (fraction) of resources used for eMBMS service at each serving eNB.

Figure 9 focuses on the $R=256$ kbps eMBMS service and deploys $N_{\mu} = \{1, 5, 10\}$ micro base stations. From the results in the figure, we clearly see the benefit of increasing micro-cellular deployment density for energy efficiency while delivering fixed-rate service across the cell. For the case of large number of micro-cells, the cell coverage with the requested data rate is already sufficiently high resulting in the energy costs that remain nearly constant with the increase of the user density. Finally, in the figure, we also include the case of combined macro/pico deployment. We illustrate the scenario where, apart from the macro eNB, we randomly place $N_{\mu} = 3$ micro eNBs and $N_p = 6$ pico eNBs. The resulting energy costs for fixed rate $R=256$ kbps eMBMS service turns out to be similar as for the case of $N_{\mu} = 5$

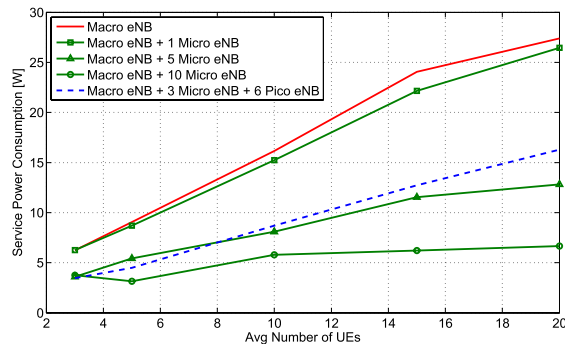


Fig. 9 Average eMBMS service power consumption for different HetNets configuration as a function of UE density ($R=256$ kbps).

micro eNBs. Thus certain level of energy costs per service channel may be obtained using different HetNets configurations.

6.3 QoE-Aware eMBMS Design

In the previous analysis, we evaluated the eMBMS channel as a fixed-rate data channel without consideration of the average video quality achievable at the UE. To this end, in the following, we introduce the Quality of Experience (QoE) as an additional requirement in the eMBMS system design. We use recently proposed QoE models for H.264/SVC services that provide analytical relations between the average data rates, $R(q, t)$, and average subjective video quality based on Mean Opinion Score (MOS), $Q(q, t)$, as a function of major H.264/SVC parameters: the frame rate (t) (Hz) and the quantization stepsize parameter (q) [30]. In this paper, we choose the rate and quality model parameters and the encoder settings, that are provided in [30] for the *Foreman* video sequence encoded using the SVC reference software [32]. Using the QoE models, we reformulate the eMBMS design problem and analyze the bandwidth and energy efficiency per unit of service in a way which is natural for mobile network operators: What are the bandwidth/energy costs per unit of eMBMS service satisfying certain average video quality threshold Q_{th} for a given eMBMS system configuration?

Figure 10 shows the bandwidth and energy cost per unit of service (video channel) as a function of video quality measured in MOS, and the achieved bit rate in the SFN-eMBMS system. As expected, the increase in the requested video quality results in higher bandwidth and energy costs per video channel and requires the availability of higher channel rates to be offered to UEs of different capabilities within the SFN-eMBMS coverage area. For example, while delivering a very high quality video services of $MOS = 4.5$ will require the availability of high bit rates channels with rates $R \geq 800$ kbps and bandwidth and energy costs of 0.9 [MHz/channel], and 8 [mJ/channel], users with capabilities to receive video services of $MOS=4.2$ will only need to receive data at bit rates $R \geq 400$ kbps, reducing the bandwidth and energy cost by almost 45% per channel.

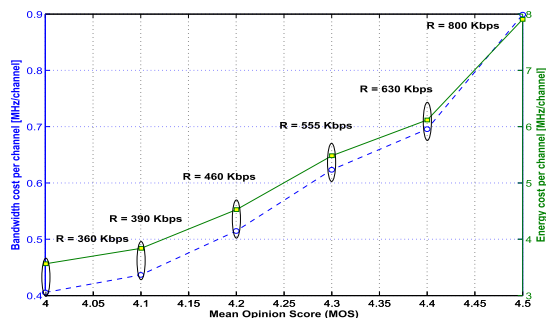


Fig. 10 Bandwidth and Energy cost per channel vs. video quality (MOS).

7. Conclusions

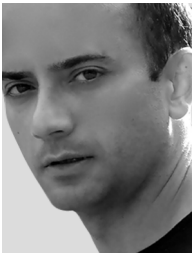
In this paper, we analysed energy efficiency of 3GPP-defined strategies for multimedia delivery in LTE/LTE-A. We presented a simple analytical approach for average service rate calculation constrained by coverage probability requirements. The average service rate results are then placed within the framework of bandwidth and energy costs per unit of service, which provides fundamental and universal metrics for bandwidth and energy efficient design of multimedia services in current and future LTE/LTE-A system configurations. As a demonstration, the proposed framework is applied on the SFN-eMBMS and the SC-eMBMS configurations, where the latter extended to upcoming Het-Nets topologies.

References

- [1] Cisco Visual Networking Index, http://www.cisco.com/en/US/netsol/ns827/networking_solutions_sub_solution.html
- [2] A. Ghosh, R. Ratasuk, B. Mondal, N. Mangalvedhe, and T. Thomas, "LTE-Advanced: next-generation wireless broadband technology," *IEEE Wireless Commun.*, vol.17, no.3, pp.10–22, June 2010.
- [3] O. Oyman, J. Foerster, T.Y.-J. Tcha, and S.-C. Lee, "Towards enhanced mobile video services over WiMAX and LTE," *IEEE Commun. Mag.*, vol.48, no.8, pp.68–76, Aug. 2010.
- [4] P. Sadeghi, R.A. Kennedy, P.B. Rapajic, and R. Shams, "Finite-state Markov modeling of fading channels: A survey of principles and applications," *IEEE Signal Process. Mag.*, vol.57, pp.57–80, Sept. 2008.
- [5] ETSI TS 26.346 v10.1.0 (Rel. 10), UMTS-Multimedia Broadcast/Multicast Service (MBMS); Protocols and Codecs, 2011.
- [6] M. Gruber and D. Zeler, "Multimedia broadcast multicast service: New transmission scheme and related challenges," *IEEE Commun. Mag.*, vol.49, no.12, pp.176–181, Dec. 2011.
- [7] A. Khandekar, N. Bhushan, J. Tingfang, and V. Vanghi, "LTE-advanced: Heterogeneous networks," *European Wireless EW 2010*, pp.978–982, Lucca, Italy, April 2010.
- [8] 3GPP TR 36.913V8.0.1 (Release 8), Requirements for further advancements for E-UTRA, March 2009.
- [9] A. Larmo, M. Lindstrom, M. Meyer, G. Pelletier, J. Torsner, and H. Wiemann, "The LTE link-layer design," *IEEE Commun. Mag.*, vol.47, no.4, pp.52–59, April 2009.
- [10] H. Holma and A. Toskala, *LTE for UMTS: Evolution to LTE-Advanced*, 2nd ed., Wiley, 2011.
- [11] ETSI TS 26.247 v11.0.0 (Rel. 11), Transparent end-to-end Packet-switched Streaming Service (PSS); Progressive Download and Dy-

amic Adaptive Streaming over HTTP (3GP-DASH), 2012.

- [12] F. Gabin, M. Kampmann, T. Lohmar, and C. Priddle, "3GPP mobile multimedia streaming standards," *IEEE Signal Process. Mag.*, vol.27, no.6, pp.134–138, 2010.
- [13] K.J. Ma, R. Bartos, S. Bhatia, and R. Nair, "Mobile video delivery with HTTP," *IEEE Commun. Mag.*, vol.49, no.4, pp.166–175, 2011.
- [14] M. Sawahashi, Y. Kishiyama, A. Morimoto, D. Nishikawa, and M. Tanno, "Coordinated multipoint transmission/reception techniques for LTE-advanced," *IEEE Wireless Commun.*, vol.17, no.3, pp.26–34, June 2010.
- [15] ETSI TS 23.246 v11.0.0 (Rel. 11)—Multimedia Broadcast/Multicast Service (MBMS); Architecture and functional description, 2012.
- [16] H.S. Wang and N. Moayeri, "Finite-state Markov channel: A useful model for radio communication channels," *IEEE Trans. Veh. Technol.*, vol.44, no.1, pp.163–171, May 1995.
- [17] Q. Zhang and S. Kassam, "Finite-state Markov model for rayleigh fading channels," *IEEE Trans. Commun.*, vol.47, no.11, pp.1688–1692, Nov. 1999.
- [18] <http://www.nt.tuwien.ac.at/ltesimulator/>
- [19] J.G. Andrews, F. Baccelli, and R.K. Ganti, "A tractable approach to coverage and rate in cellular networks," *IEEE Trans. Commun.*, vol.59, no.11, pp.3122–3134, Nov. 2011.
- [20] S. McLaughlin, P.M. Grant, J.S. Thompson, H. Hass, D.I. Laurenson, C. Khirallah, Y. Hou, and R. Wang, "Techniques for improving cellular radio base station energy efficiency," *IEEE Commun. Mag.*, vol.18, no.5, pp.10–17, Oct. 2011.
- [21] The EU FP7-ICT EARTH Project, <http://www.ict-earth.eu/>
- [22] C. Khirallah, J.S. Thompson, and H. Rashvand, "Energy and cost impact of relay and femtocell deployments in LTE-advanced," *IET Commun.*, vol.5, no.18, pp.2617–2628, Dec. 2011.
- [23] O. Arnold, F. Richter, G. Fettweis, and O. Blume, "Power consumption modeling of different base station types in heterogeneous cellular networks," *Future Network and Mobile Summit*, Florence, Italy, June 2010.
- [24] C. Khirallah and J.S. Thompson, "Energy efficiency of heterogeneous networks in LTE advanced," *J. Sig. Proc. Sys.*, vol.69, no.1, pp.105–113, Oct. 2012.
- [25] O. Arnold, F. Richter, G. Fettweis, and O. Blume, "Power consumption modeling of different base station types in heterogeneous cellular networks," *IEEE Future Network and Mobile Summit*, 2010.
- [26] S. Tombaz, P. Monti, K. Wang, A. Vastberg, M. Forzati, and J. Zander, "Impact of backhauling power consumption on the deployment of heterogeneous mobile networks," *IEEE GLOBECOM 2011*, Dec. 2011.
- [27] 3GPP R1-070984 by Nokia, "Efficiency comparison of MBMS transmission modes," Feb. 2007.
- [28] 3GPP R1-071049 by Ericsson, "Spectral efficiency comparison of possible MBMS transmission schemes: Additional results," Feb. 2007.
- [29] 3GPP R1-071433 by Motorola, "Additional results on eMBMS transmission," March 2007.
- [30] Z. Ma, M. Xu, Y.-F. Ou, and Y. Wang, "Modeling of rate and perceptual quality of compressed video as functions of frame rate and quantization stepsize and its applications," *IEEE Trans. Circuits Syst. Video Technol.*, vol.22, no.5, pp.671–682, May 2012.
- [31] H. Schwarz, D. Marpe, and T. Wiegand, "Overview of the scalable video coding extension of the H.264/AVC standard," *IEEE Trans. Circuits Syst. Video Technol.*, vol.17, pp.1103–1120, Sept. 2007.
- [32] Joint Scalable Video Model (JSVM), JSVM Software, document JVT-X203, Joint Video Team, Geneva, Switzerland, June 2007.



Chadi Khirallah received his Ph.D. degree in advanced mobile communication systems from the University of Lancaster, U.K., in 2006. He was an Assistant Researcher from 2007/2010 on the EPSRC project titled “distributed source coding for wireless video applications”, at the University of Strathclyde, Glasgow, U.K. Currently Dr. Khirallah holds the position of Senior Research Fellow at the University of Edinburgh. He served as a TPC member for many IEEE conferences including IEEE

ICME, WCNC, ICC, and VTC. His research interests include Multimedia applications over wireless networks, Energy Efficient architectures and deployment techniques in Green cellular Networks, Multihop relaying, MIMO concepts, Heterogeneous Networks, Network Coding in 4G and beyond. He has published over 45 papers in leading international journals and conference proceedings.



John Thompson was appointed as a lecturer at what is now the School of Engineering at the University of Edinburgh in 1999 where he is now full professor. He was recently promoted to a personal chair in Signal Processing and Communications. His research interests currently include signal processing, energy efficient communications systems, and multihop wireless communications. He has published over 200 papers to date including a number of invited papers, book chapters and tutorial talks, as well as

co-authoring an undergraduate textbook on digital signal processing. During 2012–2014 he will serve as member-at-large for the Board of Governors of the IEEE Communications Society. He was technical programme co-chair for the IEEE Globecom Conference in Miami in 2010 and will serve in the same role for the IEEE Vehicular Technology Conference Spring in Dresden in 2013.



Dragan Rastovac received Dipl.-Ing, Mr.-Ing. degrees in electrical engineering from the University of Novi Sad, Serbia, in 2002, 2010, respectively, where he is currently working towards Dr.-Ing degree. Since 2008, he is teaching assistant with the Department of Faculty of Education, University of Novi Sad. His research interests are in the area of information theory and coding theory with applications in multimedia delivery over wireless networks, energy efficient architectures and deployment techniques in Het-

erogeneous Networks, network coding, 4G and beyond.



Dejan Vukobratović received Dr.-Ing. degree in electrical engineering from the University of Novi Sad, Serbia, in 2008. Since then he has been an Assistant Professor with the Department of Power, Electronics and Communication Engineering, University of Novi Sad. From June 2009 until December 2010, he was on leave as Marie Curie Intra European Fellow at the University of Strathclyde, Glasgow, U.K. From 2011 2014 his research is supported by Marie Curie European Reintegration Grant. His

research interests include sparse-graph codes, iterative decoding and network coding with applications in multimedia communications and wireless sensor networks.